Closed-loop Prevention of Hypotension in the Heartbeating Brain-dead Porcine Model

Soltesz, Kristian; Sturk, Christopher; Paskevicius, Audrius; Liao, Qiuming; Qin, Guangqi; Sjöberg, Trygve; Steen, Stig

Published in:
IEEE Transactions on Biomedical Engineering

DOI:
10.1109/TBME.2016.2602228

2017

Document Version:
Peer reviewed version (aka post-print)

Closed-loop Prevention of Hypotension in the Heartbeating Brain-dead Porcine Model

Kristian Soltesz, Christopher Sturk, Audrius Paskevicius,
Qiuming Liao, Guangqi Qin, Trygve Sjöberg, and Stig Steen

***Abstract*— *Objective:* The purpose of this paper is to demonstrate feasibility of a novel closed-loop controlled therapy for prevention of hypertension in the heartbeating brain-dead porcine model. *Methods:* Dynamic modeling and system identification were based on *in vivo* data. A robust controller design was obtained for the identified models. Disturbance attenuation properties, and reliability of operation of the resulting control system, were evaluated *in vivo*. *Results:* The control system responded both predictably and consistently to external disturbances. It was possible to prevent mean arterial pressure to fall below a user-specified reference throughout 24 h of completely autonomous operation. *Conclusion:* Parameter variability in the identified models confirmed the benefit of closed-loop controlled administration of the proposed therapy. The evaluated robust controller was able to mitigate both process uncertainty and external disturbances. *Significance:* Prevention of hypertension is critical to the care of heartbeating brain-dead organ donors. Its automation would likely increase the fraction of organs suitable for transplantation from this patient group.**

***Index Terms*—Drug delivery, Medical control systems**

I. Introduction

This work is motivated by the global shortage of donor organs, suitable for transplantation [1], [2]. Most diseased organ donors are heartbeating brain-dead (BD) patients, under intensive care when brain death is diagnosed. International statistics are published annually by the Council of Europe [2].

The pathophysiology of the BD patient involves an initial domination of the parasympathetic system, resulting in bradycardia, followed by a massive sympathetic activity triggered by catecholamines released from the sympathetic nerve terminals and the adrenal gland. This is referred to as the autonomic storm, and results in a period of hypertension, as shown in Figure 1. The hypertension associated with the catecholamine storm is followed by hypotension, and often circulatory collapse. If left untreated, adequate perfusion of organs is lost, resulting in ischemia, which renders the organs unsuitable for transplantation [3]. A comprehensive summary of the pathophysiological evolution of the BD patient is found in [4]. An *in vivo* porcine study presented in [5], shows promising results of a novel pharmacological therapy aimed at achieving hemodynamic stability in BD patients. The therapy consists of intravenous infusion of a drug cocktail, consisting of noradrenaline (0.02 mg/ml), adrenaline (0.02 mg/ml), cocaine (0.02 mg/ml), thyroid hormones T3 (0.006 mg/ml) and T4 (0.006 mg/ml), anti-diuretic hormone (desmopressin) (0.72 μg/ml[1]), and cortisol (6 mg/ml).

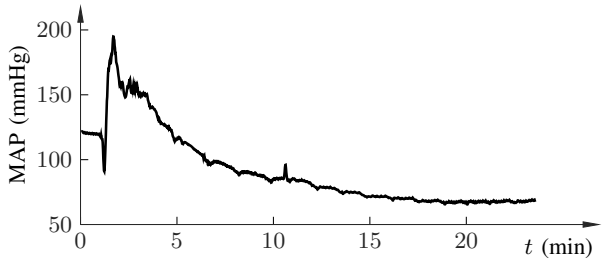

Figure 1: Hypertension caused by catecholamine storm, recorded during the study described in Section III.

In current practice, normotension of BD donors is accomplished through administering noradrenaline or other vasoconstrictors in combination with forced fluid infusion. The latter significantly increases the risk of lung oedema [4], [6], [7]. However, accomplishing normotension solely through high-dose administration of noradrenaline is not possible. In the brain-dead body, the sympathetic nerve terminals absorb the noradrenaline without releasing it again. Furthermore, high-dose administration of noradrenaline would decrease renal and hepar blood flow, thereby decreasing perfusion of the kidneys and the liver [5]. By co-administering cocaine, which acts as a monoamine reuptake-1 blocker, it is possible to achieve normotension with low-dose administration of noradrenaline, while limiting fluid therapy to cover basic needs [8].

The role of the adrenaline is to prevent bradycardia. Anti-diuretic hormone, T3, T4, and cortisol are administered to compensate for the loss of pituitary gland function [5], [8]. In this paper, closed-loop controlled infusion of the mentioned cocktail is studied. Mean arterial pressure (MAP) computed from continuous invasive blood pressure measurement is controlled by means of periodic infusion rate adjustments.

There are several reasons for pursuing robust closed-loop controlled infusion of the cocktail. Foremost, it removes the need for intermittent manual infusion rate adjustments. (Swedish[2] recommendations [9], based on [10] and [11], promote stabilization of BD potential donors for 24 h.) Closed-loop control enables automatic attenuation of disturbances,

K. Soltesz is with the Department of Automatic Control, Lund University, Lund, Sweden e-mail kristian@control.lth.se

C. Sturk is with Karolinska Institutet School of Medicine, Sweden

A. Paskevicius, Quiming Liao, Guangqi Qin, T. Sjöberg, and S. Steen are with the Department of Cardiothoracic Surgery, Lund University and Skåne University Hospital, Lund, Sweden

[1]The mass unit was erroneously reported as being mg in [5].

[2]The authors are practicing in Sweden. International regulations vary, but are of similar nature.

i.e., changes in the MAP, not explained by infusion of the cocktail, and tracking of a user specified MAP reference. Furthermore, the closed-loop system can be designed to handle inter-individual differences in pharmacokinetics and pharmacodynamics, as well as time varying behavior within a given individual.

The main novelty of this work lies in that of the application. Models for response dynamics of the mentioned cocktail, based on *in vivo* porcine data, are presented. A robust controller, based on these models, is conceived, and its efficiency is demonstrated *in vivo*. The results are discussed, and used as a basis for suggesting future work.

Although clinical impact is yet limited, closed-loop controlled drug infusion has been studied for several applications. Most notably, there is an ongoing pursuit of an artificial pancreas, with the potential to significantly facilitate the lives of diabetics. Another application which has received significant attention from the control community is anesthesia. Reviews of these two application areas, with a clinical focus, are found in [12] and [13], respectively.

The literature also contains examples, where regulation of blood pressure through closed-loop controlled drug infusion has been attempted for a number of purposes. In the 1990s, several research groups were pursuing closed-loop controlled prevention of hypertension to be used foremost in the context of heart surgery. Two representative examples are found in [14], [15]. More recently, the idea of using the MAP as a surrogate measure of analgesic effect, and to guide the closed-loop administration of synthetic opioids during general surgical procedures, has been attempted [16], [17]. A third application area has been the prevention of hypotension during caesarean section [18]. These and similar studies have had varied outcomes, and to date, there exist no clinically wide-spread devices or methods for closed-loop controlled hemodynamic stabilization.

This paper is organized as follows: Equipment and clinical protocol are described in Section II and Section III, respectively. Drug response modeling and parameter identification is the topic of Section IV, while controller structure and synthesis is discussed in Section V. Results are presented in Section VI, and discussed in Section VII.

II. Equipment

A schematic drawing of the utilized closed-loop control system is shown in Figure 2. Actuation is handled by a Carefusion Alaris TIVA infusion pump (BD, Franklin Lakes, NJ). Continuous invasive arterial pressure readings were collected using a DTXPlus blood pressure transducer (Argon Medical, Plano, TX). The transducer signal was amplified and digitized using in-housed developed circuitry. Control, hardware communications over RS232 and human-machine-interface (HMI) were implemented in the Python programming language on a standard IBM PC, running a Linux operating system. Pump communication was established by implementing the Alaris Syringe Pump Communications Protocol [19].

Apart from the experiment-specific equipment, the animals were connected to a mechanic ventilator, additional invasive blood pressure monitoring, EEG monitor, and capnograph.

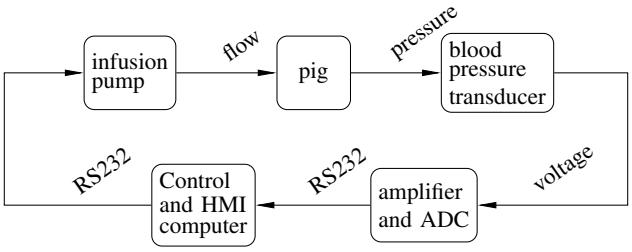

Figure 2: Block diagram showing the functional components and signals of the closed-loop control system.

III. Protocol

The conducted study comprised two experiment: one to obtain modeling data, and one to evaluate closed-loop control performance. The experiments ran under the approval M174-15, issued by the *Malmö/Lunds Regionala djurförsöksetiska nämnd* regional ethics board (REB). All animals were treated in compliance with [20], [21].

Both experiments were carried out on anesthetized adult pigs, placed in supine position. Anesthesia was induced through intramuscular injection of ketamine (30 mg/kg) and xylasin (4 mg/kg). Anesthesia, including muscle relaxation necessary for total ventilator dependency, was maintained through continuous infusion (10 ml/h) of a saline solution containing ketamine (25 mg/ml) and rocuronium (5 mg/ml). Fentanyl (4 μg/ml), midazolam (0.4 mg/kg), and atropine (0.015 mg/kg) were given intravenously before tracheotomy.

A catheter for blood pressure measurements was inserted via the right carotid artery into the ascending aorta, and continuously flushed with heparin.

During the second experiment, the animal was surgically decapitated through division of the columna between cervical vertebrae C2 and C3. Homeostasis was achieved by ligation, diathermia and surgical wax.

The animals were mechanically ventilated, using a tidal volume of 8 ml/kg and 20 breaths/min, and a positive end-expiratory pressure of 5 cmH_2O (49 kPa). Inspired oxygen fraction (FiO_2) was 0.21.

Basic fluid therapy consisting of continuous Ringer-Glucose solution (3 ml/kg/h) was administered throughout both experiments.

Nitroglycerin bolus injections (1 mg) were issued during the closed-loop controlled experiment, in order to evaluate the response of the control system to sudden blood pressure falls. In absence of controller response, a 1 mg nitroglycerin bolus would typically result in a circulatory collapse.

IV. Modeling

There exist no published pharmacokinetic or pharmacodynamic models for the distribution, metabolism, and action, of the drug cocktail [5] described in Section I. Consequently, the first activity in devising a closed-loop control system for its administration was to obtain such a model. A coarse idea about the response dynamics of the drug cocktail was available through the work behind [5], which was in terms guided by the

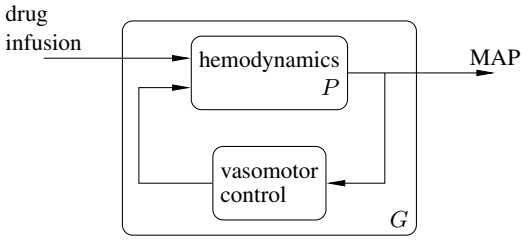

Figure 3: Block diagram illustrating the hemodynamic system to be controlled, P, and the system identified during the first experiment, G.

well-documented pharmacology of the individual components of the cocktail (cf. e.g., [22]).

Modeling experiments were performed on an anesthetized pig, with intact brain and brainstem. Consequently, the dynamics to be identified were already under feedback control by the vasomotor center, as shown in Figure 3. Using the nomenclature of the Figure 3, the obtained model describes the feedback system G, whereas the dynamics to be controlled in the BD model are those of the open-loop P. The rationale behind identifying G, was that it would demonstrate the feasibility of the experiment and identification procedure, without the need of the relatively complicated surgical procedure associated with inducing brain-death, necessary to identify P directly. If required, it would be straight-forward to repeat the identification experiment at the beginning of the closed-loop experiment involving a brain-dead pig, and update controller parameters accordingly.

The modeling experiment consisted of a series of steps and impulses (bolus doses). Each input change was issued with the system in a close to stationary state. Dosing was dimensioned to keep the MAP in, or close to, the clinically significant range of 65–100 mmHg, as prescribed by the Swedish guidelines for the treatment of heartbeating brain-dead potential donors [9]. Outcome of the step and impulse response experiments are shown in grey in Figure 4 and Figure 5, respectively.

The shape of the responses, particularity those shown in Figure 5, have the characteristics of second-order time-delayed LTI dynamics. Consequently, the model structure

$$P(s) = \frac{K}{(sT+1)(s\alpha T+1)}e^{-sL} \tag{1}$$

was asserted. Inspired by [23], the ratio between the pole locations, α, was considered fixed. Parameter identification was performed using the gradient-based method described in [24]. While DC gain K varied between the identified models, it was found that the same dynamics (α, T, L) could explain the three step responses, whereas an additional parameter set was sufficient to model the three impulse responses. Identified parameters for (1) are enlisted in Table I. The corresponding model responses are shown in black in Figure 4 and Figure 5, respectively.

It is not unusual that different pharmacokinetic parameters are used for step (infusion) and impulse (bolus) response models of the same drug. Examples for two other drugs (which have also been evaluated in closed-loop control contexts) are

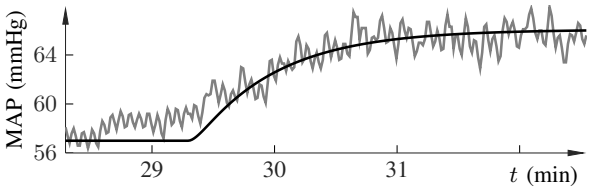

(a) Response to step from 1.5 ml/h to 4 ml/h.

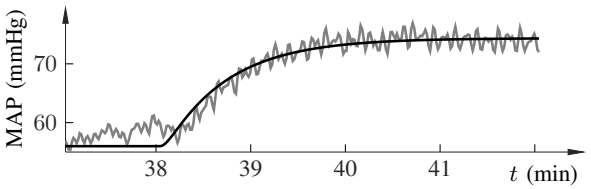

(b) Response to step from 0 ml/h to 6 ml/h.

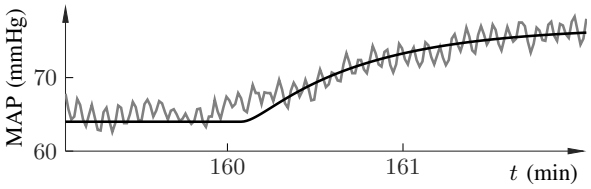

(c) Response to step from 7 ml/h to 18 ml/h.

Figure 4: Step responses (grey), and responses of identified models (black).

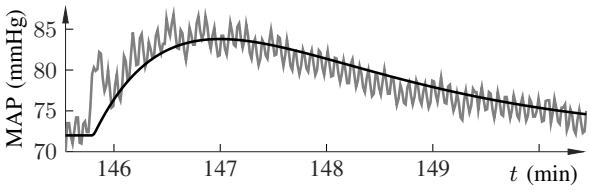

(a) Response to 0.5 ml bolus.

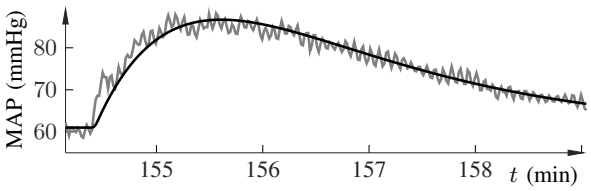

(b) Response to 1.0 ml bolus.

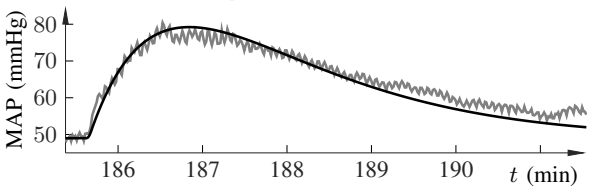

(c) Response to 1.0 ml bolus.

Figure 5: Impulse responses (grey), to bolus doses issued at 1200 ml/h rate, and responses of identified models (black).

Time series	K	T	α	L
Figure 4a	3.63	40	0.1	60
Figure 4b	3.06	40	0.1	60
Figure 4c	1.17	40	0.1	60
Figure 5a	1.28	80	0.8	15
Figure 5b	1.40	80	0.8	15
Figure 5c	1.64	80	0.8	15

Table I: Table of identified step and impulse response model parameters for the model structure (1).

found in [25] (propofol), and [26] (insulin). This indicates that the pharmacokinetics are *de facto* not LTI, but that the LTI assumption holds within each dosing regime (bolus or continuous infusion).

The variation in the DC gain parameter K within both the step and impulse response models of Table I could be partially explained by nonlinear pharmacodynamics. Typically, drugs exhibit a static nonlinear relation between effect site concentration (explained by the pharmacokinetcs) and clinical effect. This relation is often modeled by the Hill sigmoid function, introduced in [27]. The sigmoid effectively divides the effect site drug concentration into three intervals: two low-gain saturation intervals for low and high effect site concentrations, respectively, and a region of largely linear region in-between. A full investigation of nonlinear pharmacodynamics of the drug cocktail would require further experiments. For our purposes it suffices to account for the observed variation in K, disregarding its origin.

V. Controller Design

A. Structure

Many controller types have been evaluated in the context of closed-loop drug delivery. These range from simple ones, such the PID (see for example [28]), to more advanced model-based (MPC) strategies (as in for example [29]). Generally, higher fidelity models are required to benefit from more advanced controllers. Relatedly, online estimation of model parameters can be utilized to increase control performance by adaptive schemes, as suggested in for example [30], [31], [32].

The design philosophy underlying this work has been to use as simple models and controller structures as possible, and (later) only increase complexity if clinically motivated.

Given the uncertainty in the gain parameter K of (1), the design objective was to obtain a controller with robust performance over all six parameter sets of Table I. All identified models have completely damped dynamics. The step and impulse response models have normalized time delay $\tau_{step} = 0.60$ and $\tau_{impulse} = 0.22$, respectively. This indicates that robust PI or PID control are suitable choices for at least the step response models [33]. Controllers on the form

$$C(s) = k_p + k_i \frac{1}{s} + k_d s, \tag{2}$$

in series connection with a low-pass filter,

$$F(s) = \frac{1}{(T_f s + 1)^2}, \tag{3}$$

were considered. The parametrization of (2) allows for arbitrary zero placements, while being linear in the parameters. The second-order filter structure (3) was chosen to ensure high-frequency roll-off.

B. Synthesis

The design objective was to maximize low-frequency load (process input) disturbance attenuation, with constraints on closed-loop robustness. The integrated error (IE), being the time integral of the error signal e resulting from a unit load disturbance step, is a commonly used performance index. The IE has a caveat in that it can attain low values for oscillatory load responses. For non-oscillatory responses it coincides with another commonly used performance index, the integral absolute error (IAE) [33], being the $\mathcal{L}_1$-norm of e. However, the IE has a benefit over the IAE in that it is inversely proportional to the integral gain, k_i, of (2). Our design objective was therefore chosen to maximize k_i, while the obtained IAE was used to evaluate obtained performance. Robustness was enforced by simultaneously constraining the maximal peak of the sensitivity function, $S = (1 + PCF)^{-1}$, for each of the six considered instanced of P, generated by Table I. The constraint level was chosen as $M_s = 1.5$, in accordance with recommended practice [33]. Parameters of (2) were optimized by the convex optimization-based method described in [34], using a logarithmic frequency grid of 1000 points distributed between 10^{-3} rad/s (effectively zero) and the Nyquist frequency corresponding to a 1 s sample period. This sample period was deemed sufficiently short, as it gives 104 samples per arrest time for the step response models, and 159 samples per arrest time for the impulse response models [33].

C. Noise Attenuation

The time constant T_f of the low-pass filter (3) constitutes a trade-off between performance and noise sensitivity. In the total absence of filtering, corresponding to $T_f = 0$, the closed-loop noise sensitivity system $-CFS$ has infinite high-frequency gain, rendering it a poor candidate for experimental evaluation.

In order to choose an adequate filter time constant, T_f of (3), a simple noise model, $n = y - \bar{y}$, (where $\bar{y}$ denotes the mean) was derived, using a 60 s MAP sequence, y, recorded under stationary conditions. The noise model was used to drive the noise sensitivity system $-CFS$ to obtain the closed-loop control signal u_n, generated by the noise. The maximum magnitude, $\|u_n\|_\infty$, was used to quantify noise sensitivity. (Another possible choice would have been the corresponding signal energy, $\|u_n\|_2$.)

The PID parameter optimization was executed for the filtered processes FP, where F of (3) was defined through the time constant, while P represents the set of models generated by Table I. The Pareto front between performance (IAE) and

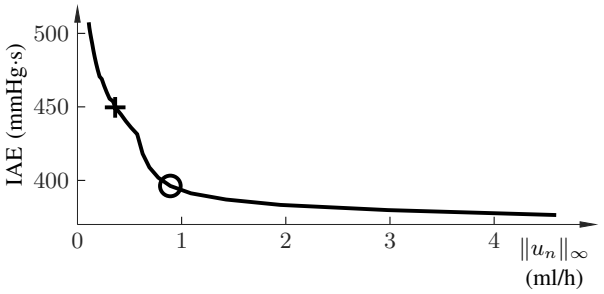

Figure 6: Pareto front between performance (IAE) and noise sensitivity ($\|u_n\|_\infty$), generated by varying the time constant T_f of (3) between 1 s and 15 s. Cross marks the PID controller evaluated *in vivo* (black in Figure 7). Circle marks the knee of the Pareto front, corresponding to $T_f = 3.5$ s).

Controller	K_p (ml/h/mmHg)	T_i (s)	T_d (s)	T_f (s)
PI (grey)	0.09	44	-	0
Filtered PID (black)	0.14	45	39	7.7

Table II: Controller and filter parameters. Colors in parenthesis refer to Figure 7.

noise sensitivity ($\|u_n\|_\infty$) shown in Figure 6 was generated by performing the optimization for T_f ranging 1-15 s. The knee of the curve, marked with a circle, corresponds to $T_f = 3.5$ s. However, the corresponding noise sensitivity, $\|u_n\|_\infty = 0.9$ ml/h, was deemed too large, and a filter with $T_f = 7.7$ s, marked with a cross, was chosen, yielding $\|u_n\|_\infty = 0.35$ ml/h.

D. Parameters and Properties

Since all obtained controllers turned out to have real zeros, the standard parallel form PID parametrization,

$$C(s) = K_p \left(1 + \frac{1}{T_i s} + T_d s\right), \tag{4}$$

can be employed. It has a benefit over (2) in that the integral time, T_i, and derivative time, T_d, have intuitive interpretations. Parameters of the considered PI and PID designs are shown in Table II, assuming the parametrizations of (4) and (3), respectively. Corresponding sensitivity functions, noise sensitivities (defined as the measurement to control signal transfer, $-CFS$), Bode diagrams and (negative) load step responses for the six considered models are shown in black (PID) and grey (PI) in Figure 7. Worst case IAE, IE, and $\|u_n\|_\infty$ values (obtained through simulation) for the considered designs are shown in Table III. It can be noted that the design was not influenced by the impulse response models – removing them from the model batch did not affect the outcome.

In order to compare the filtered PID design with what is achievable within the family of LTI controllers, a finite-

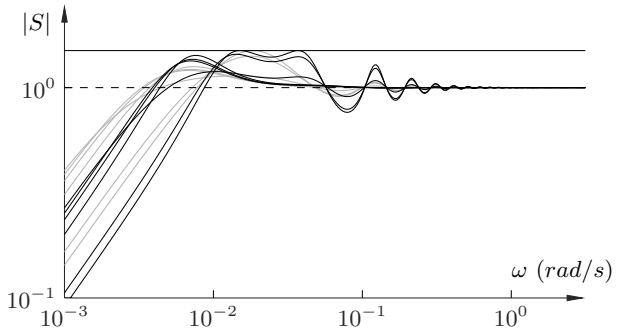

(a) Sensitivity magnitude and constraint level $M_s = 1.5$ (horizontal solid black).

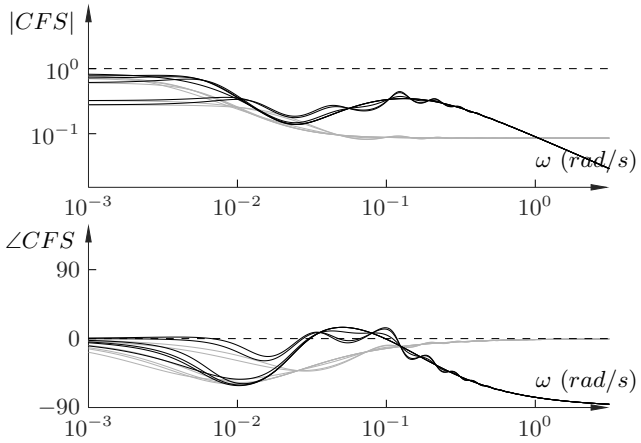

(b) Closed-loop noise sensitivity Bode diagrams.

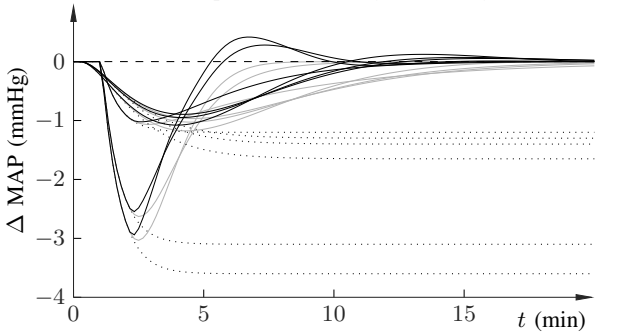

(c) Simulated closed-loop (negative) load step responses. Black lines indicate corresponding open-loop responses.

Figure 7: Simulated evaluation of PI (grey), and filtered PID (black) designs, over the six models generated by Table I.

Controller	IAE (mmHg·s)	IE (mmHg·s)	$\|u_n\|_\infty$ (ml/h)
PI (grey)	522	516	0.14
Filtered PID (black)	465	327	0.35

Table III: Load step IAE and IE and noise model induced $\|u_n\|_\infty$ for controllers presented in Section V. Colors in parenthesis refer to Figure 7. Reported values are worst cases over the models set generated by Table I.

dimensional approximation

$$Q = KS = \sum_{k=1}^{M} q_k \frac{a}{(s+a)^k}, \tag{5}$$

of the controller K, defined through the Youla parameter Q, was synthesized for the model presenting the worst case IAE under filtered PID control (first row of Table I). The sequence of stable transfer functions in (5) was defined by $a = 0.5$ rad/s, and $M = 10$. These values were heuristically chosen (close to the bandwidth of the PID controller system, and as large as possible while avoiding numeric resolution issues, respectively). The coefficients q_k were subsequently obtained by solving a convex program, minimizing the load step IAE, being the $\mathcal{L}_2$-norm of the system $P(1 - PQ)$. In order to enable a fair comparison, the sensitivity and noise sensitivity magnitudes were constrained by $\|S\|_\infty = \|1 - PQ\|_\infty \leq 1.5$ (as in the filtered PID case) and $\|Q\|_\infty \leq 1$ (which results in somewhat poorer noise attenuation than the filtered PID, but at least prevents the closed-loop from amplifying measurement noise). The optimization was carried out over the same frequency grid as used for the filtered PID synthesis. Further details on Youla parametrized synthesis can be found in for example [35].

The resulting IAE, 358 mmHg·s, was merely 23 % smaller than that of the filtered PID design, confirming the latter being a good candidate from the family of LTI controllers. This is particularly true, when considering the high order of K in (5), making it numerically ill-suited for implementation.

E. Implementation Aspects

Controllers were implemented using a sample period of 1 s, corresponding to roughly 100 samples per arrest time of the step response models. Implementation was subject to a few commonly employed practical modifications. Bumpless transfer from manual to automatic mode was implemented, as well as bumpless parameter changes [33]. Bumpless behavior was achieved by changing the integrator state whenever parameters were changes or when the controller changed from manual to automatic mode. The control signal was saturated at 0 ml/h and 15 ml/h, respectively, and integrator anti windup was achieved through clamping. The upper saturation level was later increased to 25 ml/h, as explained in Section VI. The contribution from reference changes was excluded from the derivative term, to avoid sudden control signal changes following reference changes. A setpoint weight of zero was used, to limit overshoots following reference steps. A true two-degree-of freedom design would possibly allow for further improved servo control behavior. However, the focus of the application has been regulatory control, and the subject has not been further investigated.

VI. Results

Closed-loop controller evaluation was performed *in vivo* on one pig. The experiment was divided into two phases. During the first phase, the pig was anesthetized with intact brain and brainstem. Subsequently, the pig was surgically decapitated, to obtain a heartbeating brain-dead model. The first phase was implemented to confirm adequate function of the control system under the circumstances used during the identification experiment.

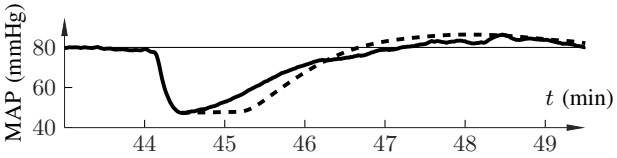

(a) *In vivo* MAP response (solid, thick), corresponding model output (dashed), and MAP reference (solid, thin).

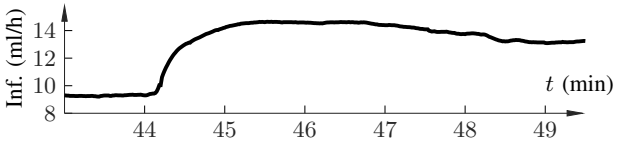

(b) Infusion rate.

Figure 8: PI controlled Response to 1 ml nitroglycerin bolus, issued at $t = 44$.

A. Intact Brain and Brainstem

The closed-loop experiment was initiated with the PI controller defined by the first row of Table II. Figure 8 (solid) shows the closed-loop response to a nitroglycerin bolus of 1 mg. Since the effect the bolus would have had in absence of closed-loop control is unknown, (it depends on the pharmacokinetics and pharmacodynamics of the nitroglycering) it is not possible to make a completely fair comparison between the experimental *in vivo* disturbance response, and that of the models of Section IV. However, given the sudden onset, as seen in Figure 8, and the comparatively slow nitroglycerin plasma half-life of 1-3 min [22], combined with the absence of vasomotor center function, we have chosen to compare the response with the gain adjusted model output generated by the *in vivo* infusion profile shown in Figure 8a (dashed). This is equivalent to asserting that the open-loop effect of the nitroglycerin bolus would have been a negative step in the MAP. As seen in Figure 8a, the *in vivo* and model responses have similar settling time, overshoot, and overall appearance. Consequently, the simple PI controller was exchanged for the filtered PID controller, defined through the third row of Table II, and the procedure was repeated with the outcome shown in Figure 9. During this part of the experiment, the infusion rate saturation of 15 ml/h was reached. It was manually changed to 25 ml/h during the ongoing experiment, which explains the flat section followed by a step in Figure 9b. Again, the *in vivo* response (solid) and model output (dashed), showed sufficient resemblance for us to proceed to the second phase of the experiment.

B. Brain-death

Upon surgical decapitation, the nitroglycerin bolus experiment was repeated three times, to evaluate consistency of performance. The outcomes are shown in Figure 10.

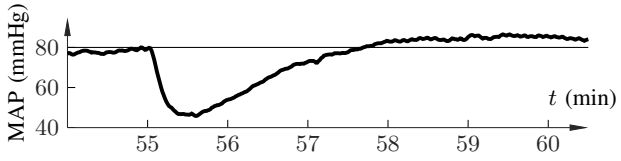

(a) *In vivo* MAP response (solid, thick), corresponding model output (dashed), and MAP reference (solid, thin).

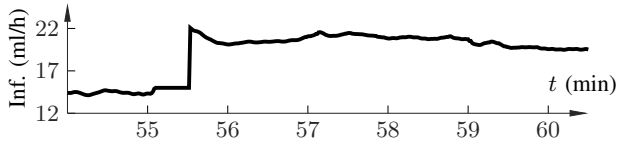

(b) Infusion rate.

Figure 9: PID controlled response to 1 mg nitroglycerin bolus, issued at $t = 55$ min.

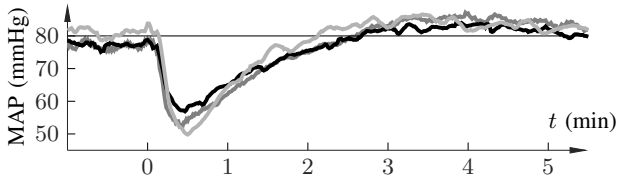

(a) *In vivo* MAP responses, and MAP reference (horizontal solid black).

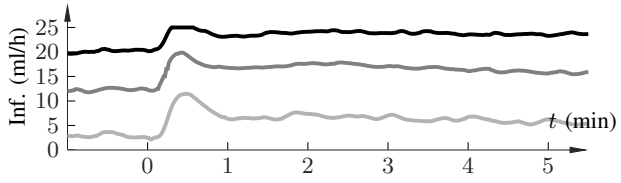

(b) Infusion rates.

Figure 10: PID controlled responses to 1 mg nitroglycerin boluses, issued at $t = 0$, corresponding to times 31 min (dark grey), 36 min (black), and 146 min (light grey) into the experiment.

Following the disturbance rejection experiments, the body was left under unattended closed-loop control for 24 h. The resulting MAP and infusion rate are shown in Figure 11. The MAP reference was 70 mmHg throughout the experiment, and the controller managed to keep the MAP above 65 mmHg during 98.5 % of the the experiment time, and above 60 mmHg during 100.0 % of the experiment time.

VII. Discussion

The herein presented study has thus constituted a successful proof of concept. However, the sample size of one limits statistical significance of further data analysis than what was presented in Section VI. The fact that the system has functioned reliably without any manual intervention throughout its first 24 h trial, is a promising fact. In the meanwhile, the results of Section VI suggest several directions of future work.

A notable shortcoming of the evaluated approach is the lack of a negative control signal. As shown in Figure 11, there

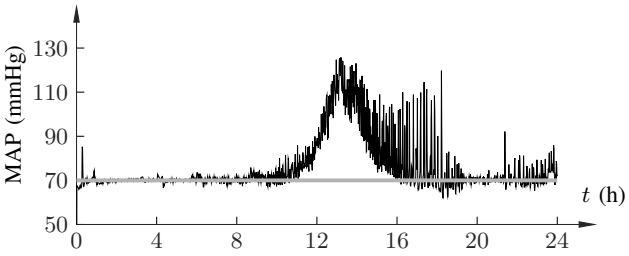

(a) *In vivo* MAP response (black), and MAP reference (grey).

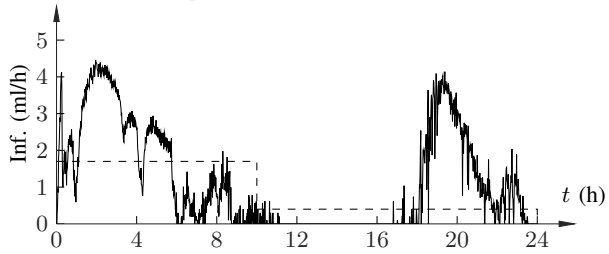

(b) Infusion rate (solid), and infusion rate used in the manually controlled study presented in [5] (dashed).

Figure 11: Unattended robust PID control during 24 h.

was a prolonged period, between 8-18 h into the experiment, during which the MAP exceeded the user-specified reference value of 70 mmHg. This period of relative hypertension was not caused by the controller, which responded correctly by halting drug infusion. The same behavior, although far from as prominent, is seen in the experimental results reported [5], [8]. A negative control signal would also be desirable during the initial catecholamine storm. During this phase, it could act to prevent pulmonary oedema caused by a characteristic increase of systemic vascular resistance (SVR), often accompanied by a decrease in pulmonary vascular resistance (PVR) [4].

A second aspect of future work is further consideration of variations in the response dynamics. These can be divided into variations over time within a given individual, and inter-individual variations. As indicated both by the results of [5], and the closed-loop controlled experiment presented herein, sensitivity to the cocktail increases over time. As a consequence, manually controlled infusion was changed from 1.7 ml/h to 0.4 ml/h after 10 h in [5]. Furthermore, the outcome of step and impulse response experiments presented in Section IV, suggest that the dynamic evolution of the responses is invariant, whereas there is a variation in steady state gain. This is also indicated very clearly by Figure 10. Consequently, there is potential for online gain estimation, and corresponding scaling of the controller DC gain, for example as proposed in [31] for a similar drug infusion control scenario. Relatedly, it can be noted that the time varying gain indicated by Figure 10 would require several subsequent manual infusion rate adjustments in absence of a closed-loop controller.

As shown in Figure 8a and Figure 9a, the dynamic response to therapy during the closed-loop experiment was predictable by the model identified using a different animal in Section IV. The most notable discrepancy between *in vivo* and model

responses is the over-estimation of the delay parameter, L of (1), indicated by Figure 8a and Figure 9a. Typically, delay over-estimation results from approximation of higher-order dynamics [33], and yields more robust PID tuning. If further studies indicate a larger mismatch, there are two possibilities. One is to increase controller robustness to encompass all expected dynamics. A second alternative is to individualize controller tuning, for instance using the method suggested in [32].

A first step toward evaluation on human heartbeating brain-dead organ donors, would be a study comprising cases of manual administration of the cocktail presented in [5] on BD patients. This would serve the purposes of validating the results from the porcine studies, as well as providing modeling data for possible adjustment of controller tuning.

VIII. Conclusion

A method for closed-loop controlled prevention of hypotension has been proposed. Feasibility of a robustly tuned filtered PID controller was confirmed by the outcome of an *in vivo* experiment, and *in silico* comparison with a Youla parameterized design. The *in vivo* experiment demonstrated both adequate disturbance attenuation and long duration (24 h) reliability of the control system. The benefit of closed-loop controlled drug administration, over open-loop feed-forward strategies such as target controlled infusion (TCI), is evident from the inter-subject variability in sensitivity to the therapy, as seen in Figure 10.

Acknowledgment

The work has been supported by the Swedish Innovation agency VINNOVA, and by the Swedish Research Council through the LCCC and ELLIIT centra.

References

[1] M. J. Irving, *et al.*, "Factors that influence the decision to be an organ donor: a systematic review of the qualitative literature," *Nephrology dialysis transplantation*, vol. 27, no. 6, pp. 2526–2533, 2011.

[2] European Directorate for the Quality of Medicines & HealthCare (EDQM), "Newsletter transplant – international figures on donation and transplantation 2014," Council of Europe, Tech. Rep., 2015, volume 20.

[3] J. Pratschke, *et al.*, "Brain death and its influence on donor organ quality and outcome after transplantation," *Transplantation*, vol. 67, no. 3, pp. 343–348, 1999.

[4] A. M. Ranasinghe and R. S. Bonser, "Endocrine changes in brain death and transplantation," *Best Practice & Research Clinical Endocrinology & Metabolism*, vol. 25, no. 5, pp. 799–812, 2011.

[5] S. Steen, *et al.*, "Pharmacological normalization of circulation after acute brain death," *Acta Anaestesiologica Scandinavica*, vol. 56, no. 8, pp. 1006–1012, 2012.

[6] S. Steen, *et al.*, "First human transplantation of a nonacceptable donor lung after reconditioning ex vivo," *The annals of thoracic surgery*, vol. 83, no. 6, pp. 2191–2194, 2007.

[7] G. Bozovic, *et al.*, "Circulation stabilizing therapy and pulmonary high-resolution computed tomography in a porcine brain-dead model," *Acta Anaesthesiologica Scandinavica*, vol. 60, pp. 93–102, 2016.

[8] S. Steen, *et al.*, "Safe orthopic transplantation of hearts harvested 24 hours after brain death and preserved for 24 hours," *Scandinavian Cardiovascular Journal*, vol. 50, no. 3, pp. 193–200, 2016.

[9] Svensk Förening för Anestesi och Intensivvård, "Vård och behandling av organdonator på intensivvårdsavdelning," www.sfai.se/riktlinje/intensivvard-av-organdonator, Downloaded 2016-05-30, Tech. Rep., 2015.

[10] McKeown, D. W. and Bonser, R. S. and Kellum, J. A., "Mangement of the heartbeating brain-dead organ donor," *British Journal of Anaesthesia*, vol. 108, no. 1, pp. 96–107, 2012.

[11] European Directorate for the Quality of Medicines & HealthCare (EDQM), "Guide to the quality and safety of organs for transplantation," Council of Europe, Tech. Rep., 2013, 5th Edition.

[12] B. W. Bequette, "Challenges and recent progress in the development of a closed-loop artificial pancreas," *Annual Reviews in Control*, vol. 36, no. 2, pp. 255–266, 2012.

[13] G. A. Dumont and J. M. Ansermino, "Closed-loop control of anesthesia: A primer for anesthesiologists," *Anesthesia & Analgesia*, vol. 117, no. 5, pp. 1130–1138, 2013.

[14] S. McKinley, *et al.*, "Clinical evaluation of closed-loop control of blood pressure in seriously ill patients," *Critical Care Medicine*, vol. 19, no. 2, pp. 166–170, 1991.

[15] S. A. A. P. Hoeksel, *et al.*, "Automated infusion of nitroglycering to control arterial hypertension during cardiac surgery," *Intensive Care Med*, vol. 22, no. 7, pp. 688–693, 1996.

[16] A. Gentilini, *et al.*, "A new paradigm for the closed-loop intraoperative administration of analgesics in humans," *IEEE Transactions on Biomedial Engineering*, vol. 49, no. 4, pp. 289–299, 2002.

[17] M. Luginbühl, *et al.*, "Closed-loop control of mean arterial blood pressure during surgery with alfentanil," *Anesthesiology*, vol. 105, no. 3, pp. 462–470, 2006.

[18] B. L. Sng, *et al.*, "Closed-loop double-vasopressor automated system vs manual bolus vasopressor to treat hypotension during spinal anaesthesia for caesarean section: a randomised controlled trial," *Anaestheisa*, vol. 69, no. 1, pp. 37–45, 2014.

[19] Cardinal Health, "Alaris syringe pump communications protocol," Tech. Rep., 2006, publication 1000PB01088 Issue 4.0.

[20] National Research Council of the National Academies, "Guide for the care and use of laboratory animals," www.nap.edu, Downloaded: 2016-05-25, Institute for Laboratory Animal Research, Tech. Rep., 2011, 8th Edition.

[21] The European Parliament, "On the protection of animals used for scientific purpose," Council of Europe, Tech. Rep., 2010, directive 2010/63/EU.

[22] J. G. Hardman, *et al.*, Eds., *Goodman & Gilman's The pharmacological basis of therapeutics*, 9th ed. New York: McGraw-Hill, 1995.

[23] M. da Silva, *et al.*, "Nonlinear identification of a minimal neuromuscular blockade model in anesthesia," *IEEE Transactions on Control Systems Technology*, vol. 20, no. 1, pp. 181–188, 2012.

[24] K. Soltesz, *et al.*, "Transfer function parameter identification by modified relay feedback," in *American Control Conference*, Baltimore, MD, 2010, pp. 2164–2169.

[25] J. Schüttler and H. Ihmsen, "Population pharmacokinetics of propofol: a multicenter study," *anesthesiology*, vol. 92, no. 3, pp. 727–738, 2000.

[26] T. Kobayashi, *et al.*, "The pharamcokinetics of insulin after continuous subcutaneous infusion or bolus subcutaneous injection in diabetic patients," *Diabetes*, vol. 32, no. 4, pp. 331–336, 1983.

[27] A. V. Hill, "The possible effects of the aggregation of the molecules of hæmoglobin on its dossociation curves," *Journal of Physiology*, vol. 40, 1910, supplement IV–VII.

[28] N. West, *et al.*, "Robust closed-loop control of induction and maintenance of propofol anesthesia," *Pediatric Anesthesia*, vol. 23, no. 8, pp. 712–719, 2013.

[29] I. Nascu, *et al.*, "Advanced model-based control studies for the induction and maintenance of intravenous anaesthesia," *IEEE Transactions on Biomedical Engineering*, vol. 62, no. 3, pp. 832–841, 2015.

[30] Z. T. Zhusubaliyev, *et al.*, "Bifurcation of analysis of PID-controlled neuromuscular blockade in closed-loop anesthesia," *Journal of Process Control*, vol. 25, pp. 152–163, 2015.

[31] J. Hahn, *et al.*, "Adaptive IMC control for drug infusion for biological systems," *Control Engineering Practice*, vol. 10, no. 1, pp. 45–56, 2002.

[32] K. Soltesz, *et al.*, "Individualized closed-loop control of propofol anesthesia: A preliminary study," *Biomedical Signal Processing and Control*, vol. 8, no. 6, pp. 500–508, 2013.

[33] K. J. Åström and T. Hägglund, *Advanced PID Control*. Research Triangle Park, NC 22709: ISA .. The instrumentation, Systems, and Automation Society, 2006.

[34] K. Soltesz, *et al.*, "A synthesis method for automatic handling of inter-patient variability in closed-loop anesthesia," in *American Control Conference*, Boston, 2016.

[35] S. P. Boyd and C. Barratt, *Linear controller design: limits of performance*. Englewood Cliffs, NJ: Prentice Hall, 1991.